International Journal of Mass Spectrometry 279 (2009) 134–146

Contents lists available at ScienceDirect

International Journal of Mass Spectrometry

journal homepage: www.elsevier.com/locate/ijms

A new broadly tunable (7.4–10.2 eV) laser based VUV light source and its first application to aerosol mass spectrometry

S.J. Hanna[a], P. Campuzano-Jost[a,*], E.A. Simpson[a], D.B. Robb[a], I. Burak[b], M.W. Blades[a], J.W. Hepburn[a], A.K. Bertram[a]

[a] Department of Chemistry, University of British Columbia, Vancouver, BC V6T 1Z1, Canada
[b] Department of Chemistry, Tel Aviv University, Tel Aviv, Israel

ARTICLE INFO

Article history:
Received 11 July 2008
Received in revised form 28 October 2008
Accepted 28 October 2008
Available online 12 November 2008

Keywords:
Vacuum ultraviolet light
Aerosol mass spectrometry
Photoionization efficiency

ABSTRACT

A laser based vacuum ultraviolet (VUV) light source using resonance enhanced four wave difference mixing in xenon gas was developed for near threshold ionization of organics in atmospheric aerosol particles. The source delivers high intensity pulses of VUV light (in the range of 10^{10} to 10^{13} photons/pulse depending on wavelength, 5 ns FWHM) with a continuously tunable wavelength from 122 nm (10.2 eV) to 168 nm (7.4 eV). The setup allows for tight (<1 mm^2) and precise focusing (μrad pointing angle adjustability), attributes required for single particle detection. The generated VUV is separated from the pump wavelengths by a custom monochromator which ensures high spectral purity and minimizes absorptive losses. The performance of the source was characterized using organic molecules in the gas phase and optimal working conditions are reported. In the gas phase measurements, photoionization efficiency (PIE) curves were collected for seven different organic species with ionization energies spanning the full wavelength range of the VUV source. The measured appearance energies are very close to the literature values of the ionization energies for all seven species. The effectiveness of the source for single particle studies was demonstrated by analysis of individual caffeine aerosols vaporized by a pulsed CO_2 laser in an ion trap mass spectrometer. Mass spectra from single particles down to 300 nm in diameter were collected. Excellent signal to noise characteristics for these small particles give a caffeine detection limit of 8×10^5 molecules which is equivalent to a single 75 nm aerosol, or approximately 1.5% of a 300 nm particle. The appearance energy of caffeine originating from the aerosol was also measured and found to be 7.91 ± 0.05 eV, in good agreement with literature values.

1. Introduction

Single photon ionization (SPI) using vacuum ultraviolet (VUV) light is a very effective soft ionization method for analytical mass spectrometry. It has been used in measurements as diverse as diagnostics of automobile exhaust [1,2], analysis of amino acids [3], and monitoring of waste incineration flue gas [4]. Unlike multiphoton ionization, no intermediate molecular resonances are required, making SPI a universal ionization technique [5]. As long as the photon energy is higher than the ionization energy of the molecule of interest, ionization will occur. Many SPI sources operate at a fixed photon energy, but tunable sources have many advantages. They allow the photon energy to be set very close to the ionization threshold minimizing fragmentation. In addition, a tunable source makes it possible to differentiate mixtures by the appearance energies of the components. A tunable source also makes it possible to measure ionization energies (IEs). Having both the IE and the SPI mass spectrum of the molecule is a powerful combination for product identification in analytical applications.

Pulsed lasers are an excellent source of VUV light. Unlike synchrotrons, they are laboratory based instruments, and although considerably more complex than discharge lamps, they can produce high intensity pulses of coherent radiation. The coherent light from a laser source has several advantages. It is highly collimated and can be steered over considerable distances by conventional optics. In addition the bandwidth can be very narrow, the spectral purity can be high, and the polarization can be easily controlled. There is also no higher order VUV radiation which can be an issue with synchrotron undulator sources [6]. Pulsed lasers sources are also well suited for measuring discreet events, such as in pump-probe experiments or single particle mass spectrometry.

* Corresponding author. Tel.: +1 604 822 3296; fax: +1 604 822 2847.
E-mail addresses: pcampuzano@chem.ubc.ca (P. Campuzano-Jost), blades@chem.ubc.ca (M.W. Blades), hepburn@chem.ubc.ca (J.W. Hepburn), bertram@chem.ubc.ca (A.K. Bertram).

1387-3806/$ – see front matter © 2008 Elsevier B.V. All rights reserved.
doi:10.1016/j.ijms.2008.10.024

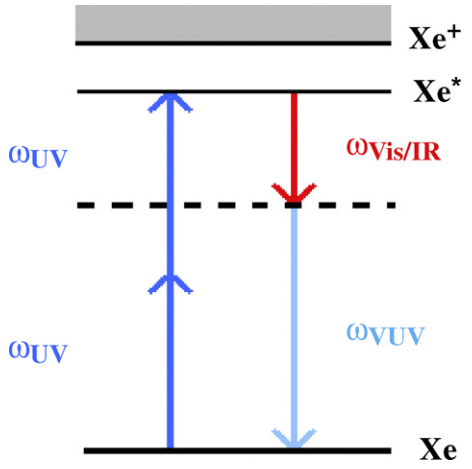

Fig. 1. Schematic of resonance enhanced four wave difference mixing in xenon gas.

Continuously tunable laser based VUV light sources capable of scanning over a wide frequency range are predominantly based on four wave sum or difference mixing in rare gases or metal vapors. Here three applied frequencies of light are used to produce a fourth based on the non-linear response of a gas phase medium [6–8]. Resonance enhanced four wave mixing increases the VUV output by having two of the applied frequencies set to reach a two-photon resonance in the medium. The third applied frequency is tunable and allows tunable VUV to be generated [6,7,9]. This is shown schematically in Fig. 1.

The majority of tunable VUV sources based on four wave mixing use two dye lasers. One of the lasers has its output fixed at the wavelength of the two-photon resonance, and the other is scanned to produce tunable output. In these systems tuning over a wide range of VUV energies requires frequent dye changes, which is time consuming and not suitable for rapid and routine analysis. For example, Hilber et al. used thirteen different dyes to produce VUV light between 127 nm and 147 nm [10]. Some variations on the two dye laser scheme have been employed. Faris et al. used a combination of a dye laser and an ArF excimer laser, although dye changes were still required in order to scan over a broad frequency range [11]. Alternatively, Qi and McIlroy used two OPOs pumped by separate Nd:YAG lasers [12], a system which overcomes the necessity of frequent dye changes.

A serious concern in analytical applications of VUV generated by four wave mixing is spectral purity. The generated light will contain the residual high intensity UV and visible or IR radiation used for the four wave mixing process, which are typically 6–8 orders of magnitude more intense than the generated VUV radiation. This, particularly in the case of the UV, can lead to unwanted multiphoton ionization. To avoid these effects, the VUV must be separated from the pump frequencies. Traditional grating monochromators typically have only about 10% efficiency in the VUV, and are easily damaged by intense UV pulses. Monochromators based on refractive optics such as prisms or lenses have higher efficiencies and damage thresholds. An off-axis lens monochromator has the advantage of focusing the light and allowing optimal discrimination. This technique has been used quite extensively in experiments where 355 nm light is tripled to produce VUV radiation at 118 nm [13–16] and was reported in a tunable monochromator by Vondrasek et al. in 1988 [17]. However, no design to our knowledge has been presented that is capable of giving a precisely positioned VUV focus while scanning over a broad range of frequencies.

In this work we present a new VUV light source based on four wave difference mixing in xenon gas which incorporates both a dye laser and an OPO. The dye laser is used at a fixed frequency to access a two-photon resonance and the OPO provides the tunable wavelength. This has the advantage of allowing wavelength scanning between 122 nm and 168 nm, while requiring only one dye change. Both the dye laser and OPO produce narrow bandwidth light which allows for high resolution VUV scanning (bandwidth on the order of 0.5 cm^{-1}). In addition, a custom monochromator based on a single MgF_2 lens has been incorporated into the design to separate the generated VUV from the pump wavelengths, to ensure high spectral purity, and to minimize absorptive losses. Furthermore, the monochromator was specially designed to maintain a tight and precisely positioned focus even as the VUV wavelength is changed over tens of nanometers. Careful computer control of the pump optics and the monochromator lens allows a precisely positioned and uniformly sized focus to be maintained in the center of the ionization region while scanning. To the best of our knowledge, this is the first demonstration of a laser based VUV source that is capable of routinely scanning over this wide frequency range while maintaining a tight and precise focus and maintaining a high spectral purity.

Although our system has other potential applications, it was designed specifically as an ionization source for single particle aerosol mass spectrometry. Aerosol particles, which range in size from 2 nm to tens of microns [18], are ubiquitous in the earth's atmosphere, and a very significant mass fraction (20–90%) of the submicron aerosol component is composed of, or contains, organic molecules [19]. The composition of these organic aerosols has been shown to be extremely complex and often consists of large, fragile molecules which present a significant challenge to standard analytical techniques [20,21]. In recent years a wide variety of new instrumentation has been developed to study these particles, with one very powerful technique being aerosol mass spectrometry [22–27].

For mass spectrometric analysis of organic aerosols, ionization using traditional 70 eV electron impact leads to extensive fragmentation and complex mass spectra. To reduce this fragmentation, several groups have coupled aerosol mass spectrometers with soft ionization sources, some examples of which include low energy electron impact (PERCI) [28], chemical ionization (CI) [29,30], metal attachment [27], resonance enhanced multiphoton ionization (REMPI) [31–35], and single photon ionization.

Tripling the third harmonic of a Nd:YAG laser to produce 118 nm light has been used quite extensively in aerosol mass spectrometers [36–38]. It is a relatively simple system and gentle in comparison with many other ionization methods, although it has been shown that even 118 nm light is high enough in energy to cause significant fragmentation of organics [39]. Other avenues that have been explored include VUV lamps [40,2,41], use of a synchrotron [42–45], and resonance enhanced four wave difference mixing to give VUV light at 142 nm (8.75 eV) [39]. Recently developed rare-gas excimer lamps have been successfully deployed as photoionization sources for mass spectrometry [46,47] while the Advanced Light Source in Berkeley California has been used very effectively to characterize the products of heterogeneous reactions involving small organic aerosols [42]. However, the new rare-gas excimer lamps are cw, broadband, and not continuously tunable. The synchrotron is also cw, and access to such a facility is limited.

The first objective of this work was to develop a new, continuously tunable, laboratory based VUV light source designed specifically for single particle aerosol mass spectrometry. Our source has a high photon flux, which is a prerequisite for aerosol studies, especially for single particle studies (a 1 μm aerosol has $\sim 10^9$ molecules, ~500 fg of material). It is continuously tunable from 7.4 eV to 10.2 eV (168 nm to 122 nm) so that fragmentation can be minimized and compounds can be separated by ionization energies. A custom monochromator maintains a tight and precisely

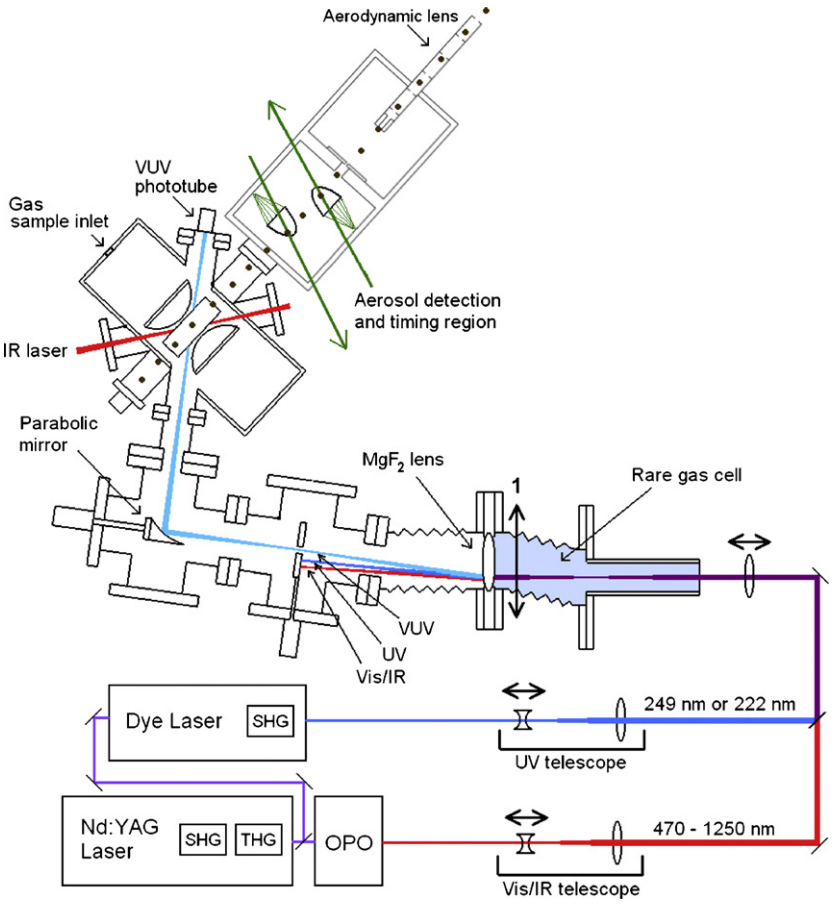

Fig. 2. Schematic of the VUV source and aerosol mass spectrometer. To generate VUV, UV light from a dye laser and visible or IR light from an OPO is focused into a rare gas cell. The UV and visible/IR light are separated from the generated VUV by an off-axis MgF_2 lens and blocked by a ceramic beam dump. The VUV light is refocused into the center of an ion trap mass spectrometer by a parabolic mirror. Aerosols are focused into a collimated stream by an aerodynamic lens and detected by scattering from two 532 nm cw Nd:YAG lasers. When a particle reaches the center of the ion trap, a CO_2 laser is fired to vaporize it, followed by single photon ionization.

positioned focus even as the VUV wavelength is changed over tens of nanometers. The source is laser based, so pulses are available on demand and mass spectra from individual aerosol particles can be acquired. In this work the development of our continuously tunable VUV source is described in detail and some gas phase measurements are reported to illustrate the sensitivity and accuracy of the combined VUV-mass spectrometer. Scanning over a wide frequency range while maintaining a tight and constant focus requires special equipment and arrangements and this detailed description should allow others to assess the usefulness of such a VUV source for different applications.

The second objective of this work was to demonstrate the performance of the VUV source in analyzing single aerosol particles Fragment free mass spectra for caffeine particles were acquired and the ionization energy of the aerosol constituent was determined. This is the first measurement of ionization energies of aerosol constituents using a laser based VUV source. The sensitivity of our system for caffeine aerosols was determined and the sensitivity for other types of organic aerosols is discussed.

2. Experimental

2.1. VUV generation and custom VUV monochromator

In this system vacuum ultraviolet light is generated by resonance enhanced four wave difference mixing in xenon gas. The output of a pulsed Nd:YAG laser (Continuum Powerlite PLUS), which produces 800 mJ per pulse at 355 nm, is split evenly and used to pump both a dye laser (Sirah PrecisionScan SL) and an optical parametric oscillator (OPO) (Continuum Sunlite). The second harmonic of the dye laser is tuned to deliver high intensity pulses (6–12 mJ) at either 249.56 nm or 222.62 nm, each of which corresponds to a separate two-photon resonance in xenon gas. The OPO is used to generate a continuously tunable output between 480 nm and 1250 nm. By focusing one of the two ultraviolet (UV) wavelengths, along with the tunable output of the OPO, into a xenon gas cell, vacuum ultraviolet light is produced by resonance enhanced four wave difference mixing. The four wave mixing process is shown schematically in Fig. 1 and its particulars have been described extensively [6,7]. Using a single laser to pump both the dye laser and the OPO eliminates timing jitter between pulses and increases the stability of the VUV output.

The OPO is capable of producing light between 445 nm and 1750 nm, but for this application the energy was too low below 480 nm and above 1250 nm to produce satisfactory amounts of VUV. These energy boundaries, together with the MgF_2 transmission cutoff at approximately 120 nm, limit our ionization source to photon energies between 7.4 eV (168 nm) and 10.2 eV (122 nm). However, this energy range is well suited for gentle ionization of a wide range of organic molecules [5,48,49]. The vast majority of organic compounds found in aerosols have ionization energies in this range, with some notable exceptions. Small acids such as acetic, formic [50], and fumaric acid [51] have IEs above 10.2 eV. Other molecules such formaldehyde [50] and peroxyacetylnitrate (PAN)

[52] are also out of reach with the current setup. VUV sources which use a jet of rare gas rather than a cell are not limited by the transmission cutoff of the windows and can produce light of up to 20 eV [53], albeit at lower intensities and with the necessity of more complex, reflective monochromators.

Fig. 2 is a schematic of the experimental setup, showing in detail the optical arrangement used to generate vacuum ultraviolet light and the custom monochromator used to separate the VUV from the UV and visible or IR light used to produce it. Also shown is the single particle aerosol mass spectrometer which is coupled to the VUV source. The aerosol mass spectrometer is described below.

As shown in Fig. 2, the pulses from the dye laser and OPO are combined using a dichroic mirror and focused together into the xenon gas cell. Because the OPO wavelengths cover such a broad range (480–1250 nm), it is necessary to use two telescopes to maintain focus matching of the UV and visible/IR in the rare gas cell. During a VUV wavelength scan the UV telescope is kept in a fixed position, while the visible/IR telescope is slowly scanned to maintain a good overlap between the foci and thus maximize the VUV intensity.

At the exit of the xenon gas cell the co-linear UV, visible/IR, and VUV beams are directed off-axis onto a MgF_2 lens which disperses the different wavelengths and allows the UV and visible/IR beams to be blocked by a ceramic plate while the VUV passes through a 3 mm pinhole and is directed into the ion trap mass spectrometer. Due to wavelength dependent changes in the refractive index of MgF_2, VUV beams of different wavelengths are deflected at different angles by the lens. To keep the deflection angle constant as the VUV wavelength is changed, the position of the MgF_2 lens is scanned in a direction perpendicular to the propagation axis of the VUV beam as shown by arrow 1 in Fig. 2.

A single lens dispersion system has several advantages over other systems. First, it minimizes absorptive losses by having a single element both disperse the light and act as a vacuum break between the rare gas cell and the high vacuum part of the system. Second, the focusing properties of the lens allow the residual pump wavelengths to be blocked at the focus of the VUV light where discrimination is optimal. The MgF_2 lens also absorbs any undesired shorter wavelengths generated by four wave sum mixing or tripling of the pump beams.

Once the VUV has been separated from the pump wavelengths, it is refocused and directed into the ion trap mass spectrometer using an off-axis parabolic mirror. For studies of aerosol particles tight focusing is necessary. In aerosol experiments submicron particles enter the mass spectrometer through a hole in the ring electrode and are vaporized by a pulsed CO_2 laser when they reach the center of the ion trap. If the resulting vapor plume is allowed to expand too far, its density and the density of photons in a beam large enough to capture the whole plume are too low to result in good ionization efficiency. On the other hand, if the detection zone becomes too small, irregularities in the particle beam as well as irregularities in the desorption and ionization beams will significantly decrease reproducibility. A good compromise is using an ionization zone of approximately 1 mm in diameter [36]. Assuming a sonic expansion of the vapor plume, this means having the ionization pulse 3–8 μs after the desorption pulse (depending on molecular mass) in order to ensure optimal overlap. Even under these conditions, good reproducibility can only be achieved by precise control of the size and position of the VUV focus. The off-axis parabolic mirror allows for tight focusing; precision positioning is achieved by mounting the vacuum chamber which houses the off-axis parabolic mirror on a precision *x*–*y* translation stage allowing micrometer level changes to be made in the horizontal position of the VUV beam. The mirror itself is mounted on a rotational vacuum feedthrough which has been adapted to allow for μrad adjustments in the vertical angle of the beam.

Because of wavelength dependent changes in the refractive index of MgF_2, the VUV focus size in the ion trap will vary as the VUV wavelength is changed. For aerosol experiments it is important that the focus size remains constant as the VUV wavelength changes so that a constant, optimized overlap of the VUV beam with the cloud of molecules from the recently vaporized aerosol particle is maintained. To achieve this, the position of the lens which focuses the pump beams into the xenon gas cell is scanned as function of VUV wavelength. This allows a constant focal volume to be maintained at the position where the VUV beam interacts with the aerosol plume.

The VUV is detected after exiting the ion trap, and its intensity is measured using a fast phototube (Hamamatsu, R1328U-54, 270 ps rise time). The photon flux is high enough to approach the damage threshold of the phototube so only the light reflected at 45 degrees from a MgF_2 window on the exit port is monitored. At wavelengths longer than 150 nm even the reflected light could saturate the phototube and a second reflector is added to further attenuate the light. Even with these precautions it is possible that the phototube is somewhat saturated above 150 nm, which could result in lower than actual photon fluxes being measured.

The VUV source can be operated in two different modes. The first is a fast scanning mode, where the VUV wavelength is scanned continuously over tens of nanometers. The second is a fixed wavelength mode with the VUV optimized at single photon energy.

2.1.1. Fast VUV scanning mode

The challenge when scanning the VUV photon energy is in maintaining a good overlap between the UV and visible/IR beams in the xenon gas cell while also maintaining a good alignment of the generated VUV through the ion trap. To make this possible in the fast scan mode, the MgF_2 lens, the visible/IR telescope, and the lens which focuses light into the rare gas cell (Fig. 2) are all mounted with motorized actuators that can be controlled remotely by a computer. This allows precise control of the VUV beam, and makes it easy to scan over large wavelength ranges. The only limitation on scanning speed is the need to change laser dyes when switching between the two xenon resonances. A scan of the full range can be completed in a few hours and, if the UV wavelength is not changed, scans over half of the range can be done in as little as thirty minutes. This quick scanning ability can be very useful for rapid compound identification using ionization energies, and it also allows the VUV wavelength to be easily optimized for any particular compound of interest. If high resolution scans are desired, the various optical elements and the OPO can be scanned very slowly. At the slowest possible scanning speed (0.002 nm/s for the OPO) the scan resolution becomes limited by the bandwidth of the VUV light (less than 0.5 cm^{-1} [54]) rather than by the scanning capabilities of the system.

Since the phase matching conditions for VUV generation are pressure dependent [6,8], careful tuning of the xenon gas pressure in the four wave mixing cell is required for optimum conversion efficiency throughout the spectrum. However, in the current setup the gas pressure is not constantly tuned when scanning quickly across long wavelength ranges. As a compromise between optimum VUV conversion efficiency and ease of scanning, several xenon pressure regimes have been determined that can be used over a range of wavelengths. These pressures are optimized for the pump energies and optical arrangement described here, and may not represent the best conditions for all systems. Table 1 shows the range of VUV wavelengths that can be generated using the two xenon resonances and the output of the OPO. Also shown are the xenon pressures used for rapid scans in the different wavelength ranges.

Table 1
Wavelength and energy ranges of vacuum UV light generated using different combinations of pump laser wavelength. Also shown are the xenon gas pressures used in the rare gas cell for VUV generation over several broad wavelength ranges.

Dye laser wavelength (nm)	OPO wavelength (nm)	VUV wavelength (nm)	VUV energy (eV)	Xe pressure in the rare gas cell (Torr)
222.56	1250–831 (Idler)	122–128.5	10.16–9.65	35
	831–710 (Idler)	128.5–132	9.65–9.40	12
	710–470 (Signal)	132–146	9.40–8.51	45
249.62	1250–1010 (Idler)	139–142	8.94–8.75	45
	1010–710 (Idler)	142–151	8.75–8.19	12
	710–470 (Signal)	151–168	8.19–7.40	25

2.1.2. Fixed VUV wavelength mode

In addition to operating in a scanning mode we can also carry out experiments in a fixed VUV wavelength mode. In this case the visible/IR wavelength is fixed, as are the positions of the visible/IR telescope and the lens which focuses light into the rare gas cell. The gas pressure and composition in the cell are optimized to give the best conversion efficiency. The conditions that lead to the best conversion efficiencies are discussed in more detail in Section 3.1.2. An advantage of this mode is the ability to increase the VUV intensity, something which can be useful in some instances. With the fast tunability of the OPO and the motorized actuators on all the stages, it is very easy to jump between VUV wavelengths when operating in this fixed VUV wavelength mode. A jump to a new wavelength tens of nanometers away can be done in just a few minutes.

2.2. Gas phase measurements

To introduce the gas phase analytes into the ion trap, a glass bubbler containing a small amount of liquid analyte was coupled to the trap manifold via a 100 μm critical orifice placed off-axis to the ion trap to ensure thermalizing of the compound prior to analysis. Several pump/thaw cycles were undertaken to degas the samples and the analyte was then cooled to a temperature that gave a vapor pressure of 50–1000 mTorr above the sample (measured by a capacitance manometer (MKS 622)). The critical orifice between the bubbler and ion trap guaranteed a stable flow into the trap. Typical analyte pressures in the ion trap were between 9 μTorr and 85 μTorr as measured by a cold cathode gauge (MKS 423). The absolute pressure reading of the cold cathode gauge was calibrated using nitrogen gas and a high accuracy absolute capacitance manometer (MKS 120). The cold cathode gauge itself was typically switched off during measurements to avoid ion production from this source.

The ion trap mass spectrometer used for these experiments has been previously described [55,56] and only a brief overview will be given here. The ion trap electrodes were built in house and mounted in a custom vacuum manifold which allows access through the center of the ring electrode and along two diagonal paths between the ring and endcap electrodes (Fig. 2). An RF quadrupole power supply (Extranuclear Laboratories, Model 011-1) modified to operate between 0.6 MHz and 3.0 MHz was tuned to 967 kHz for ion trapping. Once trapped, the ions were collisionally cooled for 10 ms in ~1 mTorr of helium gas. The ion trap was operated in mass selective instability mode and ejected ions were detected with an electron multiplier (ETP AF138). The detector signal was amplified with a shaping current amplifier (Keithley 427) and recorded on a computer using a 16 bit ADC card (NI PCI-MIO-16XE-10) controlled by custom software written in the National Instruments Labview programming environment. This card was also used to generate the RF ramp for ion ejection. Mass calibration of the ion trap was done using 70 eV electron impact of small amounts of perfluorotributylamine. Mass scans were performed at a scanning speed of 4000 Da/s, with a mass resolution under these conditions of ~500 m/Δm at 264 m/z.

2.3. Aerosol measurements

A TSI constant output atomizer (TSI Inc., Model 3076) was used to generate aerosol particles from a pure caffeine solution (~1×10^{-3} g/ml in Millipore water (18 MΩ)). The particles were size selected with a TSI DMA (TSI Inc., Model 3081) and passed through a ^{85}Kr charge neutralizer (TSI Inc., Model 3054) that also acted as drying tube, as well as a 24″ nafion diffusion dryer (MD-110, Permapure Inc.), to avoid additional drying and size changes prior to analysis.

The single particle aerosol mass spectrometer is shown schematically in Fig. 2. It consists of three distinct regions; an aerosol inlet where the particles are focused into a collimated stream by an aerodynamic lens, a particle sizing module where individual aerosols are detected by light scattering, and the analysis module consisting of the ion trap mass spectrometer and the two lasers for vaporization and ionization. The details of the aerosol inlet and light scattering module will be described in more detail in future publications [57] and only a brief overview will be given here.

In this system particles are drawn into the instrument through an aerodynamic lens which consists of a series of apertures modeled after Liu et al. [58,59]. The aerodynamic lens focuses the particles into a tight stream which then passes through a skimmer and enters the sizing region. In the sizing region, the scattered light from two 532 nm CW Nd:YAG lasers (Excelsior 532, 100 mW single mode, Spectra Physics) is detected and then used to determine the particle velocities. A particle's aerodynamic diameter can be determined from its velocity using a calibration curve generated with polystyrene latex beads of known sizes. The particle velocities are recorded by an FPGA board (PCI-7831R, National Instruments) and used to generate the laser triggers in real time. The FPGA board also records information such as the laser power and scattering signal size for the analyzed particle. With the current setup, sizing efficiencies of well over 90% are achievable for particle sizes of 400 nm and above with a minimum detectable size of ~225 nm [57]. After exiting the sizing region, the particles enter the ion trap mass spectrometer through a 2 mm hole in the ring electrode where they are vaporized, ionized, and mass analyzed.

In these experiments infrared light from a pulsed TEA-CO_2 laser (MTL-3G, Edinburgh Instruments) was used to vaporize the particles. After a fixed delay of 3 μs the aerosols were ionized with vacuum UV light and mass analyzed. A delay of 3 μs was chosen because it allowed the cloud of vapor to expand and fill the ionization volume giving the maximum ion signal. The energy of the IR and VUV pulses was measured after they exited the ion trap. For the CO_2 laser, a power meter with a thermal detector (Ophir Model 3A-SH) was used to measure the average IR power. For the VUV, a fast phototube (Hamamatsu, R1328U-54) was used to measure the single-shot energy.

For aerosol measurements the ion trap was operated in the same manner as described above for the gas phase measurements. After vaporization and ionization, the ions from an aerosol particle were stored in the trap for 10 ms to allow for collisional cooling with the

helium bath gas. After cooling, the RF voltage on the ion trap was ramped and the ions were ejected at a mass scan speed of 4000 Da/s.

2.4. Triggering the laser system; pulses on demand

The Nd:YAG laser which pumps both the dye laser and the OPO operates at 10 Hz, but the timing of each pulse can be shifted by up to 60 ms while still maintaining an average firing rate of 10 Hz. This means that the VUV pulses can be generated on demand to coincide with other aspects of an experiment, such as the arrival of an aerosol particle in the ion trap. The pulsed nature of the source makes it well suited for coupling to an ion trap mass spectrometer, which can obtain discreet mass spectra after every ionization event. In particular a pulsed source is very valuable for single particle aerosol experiments. The cloud of molecules from a vaporized particle is only in the ionization region for approximately 10 μs, and with a pulsed source the entire photon flux is delivered during this time, ensuring the maximum photoionization efficiency. With a continuous source the particle is only exposed to a fraction of the total photon flux. For example, with a synchrotron source which delivers ~10^{16} photons per second [42] a single particle which is in the ionization region for 10 μs will only see 10^{11} photons. It should be kept in mind, however, that a continuous source can have other advantages. For instance, a synchrotron source has been used very effectively to study a continuous steam of very small particles which cannot be detected individually [42,43].

2.5. Chemicals

Benzaldehyde (≥99%), ethylbenzene (99.8%), α-pinene (≥99%), and tripropyl amine (99+%) were purchased from Aldrich. Benzene (99.97%) was purchased from OmniSolve, toluene (99.9%) was purchased from Fisher, and chlorobenzene (99+%) was purchased from Acros. Caffeine (≥98.5%) was purchased from Sigma–Aldrich. All chemicals were used without additional purification. Gases were purchased from Praxair. Gases used were xenon (99.999%), argon (99.999%), krypton (99.999%), and helium (99.999%).

3. Results and discussion

3.1. VUV source characterization

3.1.1. Brightness in fast scanning mode

Fig. 3 shows the number of VUV photons detected as a function of wavelength over the entire 122–168 nm range. Between 10^{10} and 10^{13} photons are generated per 5 ns pulse. The values in Table 2 were calculated using the absolute photocathode sensitivity at 253.7 nm and a generic calibration curve from 320 nm to 115 nm which were provided by the manufacturer of the VUV phototube. A 20% error is estimated to arise from graphical interpolation of this calibration curve. In addition, since the phototube was only calibrated at 253.7 nm, there is some uncertainty in the transmission of the phototube's MgF_2 window at shorter wavelengths. For wavelengths below 130 nm, where MgF_2 begins to absorb significantly, it is estimated that the transmission may be up to 50% lower than expected. Between 130 nm and 140 nm it is estimated that the MgF_2 transmission could be up to 30% lower than expected. This would lead to an underestimation of the real photon flux in both cases.

To prevent saturation of the phototube, only the light reflected at 45 degrees off of a MgF_2 window on the exit port is monitored. The amount of light reflected was measured to be 4 ± 1% at both 148.5 nm and 131 nm leading to a 25% uncertainty in the calculated number of photons. However, due to the increasing absorbance of MgF_2, the reflection may be greater at short wavelengths [60] and for wavelengths below 130 nm it could be up to five times higher. At

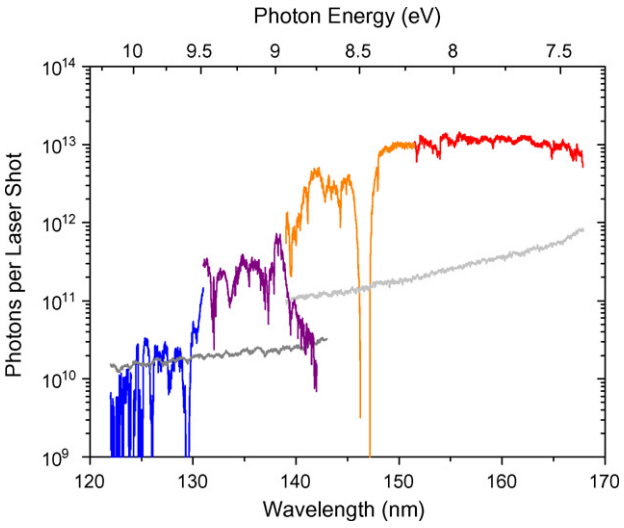

Fig. 3. Number of photons per pulse generated across the full range of the VUV source. The grey traces are UV background. The dark grey trace is UV light at 222.56 nm and the light grey is light at 249.62 nm. The change in the background at 140 nm reflects the higher UV power available when using 249.62 nm. Estimated uncertainties are listed in Table 2.

wavelengths longer than 150 nm the VUV is intense enough that a second MgF_2 reflector has to be used which introduces a further 25% uncertainty at long wavelengths. The uncertainties for the numbers reported in Fig. 3 are summarized in Table 2.

The rapid decline in VUV intensity at wavelengths below 128 nm reflects the increasing absorbance of the MgF_2 monochromator lens at short wavelengths as well as the reduced energy of the OPO as it is tuned into the IR. It has also been shown that the efficiency of four wave difference mixing decreases as the generated wavelength decreases [10]. Two sharp dropouts which occur at 129.56 nm and 146.96 nm are due to the presence of strong resonance lines in xenon gas. The refractive index of xenon changes rapidly in the vicinity of these resonance lines [61] and the phase matching conditions required for generation of VUV by four wave mixing cannot be maintained. Fig. 3 was made with the VUV system in fast scanning mode, and the xenon pressures used were relatively high (Table 1). The width of the energy dropouts around the resonances can be minimized by decreasing the xenon pressure in the rare gas cell, but this comes at the price of reduced energy at wavelengths further away from the resonance lines. The pressures listed in Table 1 are compromises which minimize the width of the dropouts without sacrificing too much power over the whole scanning range.

3.1.2. Brightness when optimizing for a single wavelength

In many experiments it is advantageous to fix the VUV at a particular wavelength while other parameters are investigated. For this mode of operation some measures can be taken to increase the VUV output, especially in the vicinity of strong resonance lines. At any wavelength the xenon pressure can be optimized to give the best VUV output. Near resonance lines, low xenon pressures generally give the best conversion efficiency and allow VUV to be generated within 0.5 nm of the resonance. In addition, on the high energy side of the resonances it is possible to achieve increased VUV conversion efficiency by adding a second, positively dispersive gas to the four wave mixing cell. This is possible because xenon shows anomalous dispersion over a short energy range just to the blue of the resonance lines [61]. The addition of a positively dispersive gas allows the xenon pressure to be increased without destruction of the phase matching conditions required to propagate the generated VUV [5,62]. However, since the refractive index changes very

Table 2
Average photons per pulse available for different VUV ranges. Also included are the estimated upper and lower limits for the photon flux based on the uncertainties discussed in Section 3.1.1.

Dye laser wavelength (nm)	Wavelength range (nm)	Energy range (eV)	Average photons	Upper limit	Lower limit
222.56	122–130	10.16–9.56	1×10^{10}	3×10^{10}	1.4×10^{9}
	130–140	9.56–8.87	2×10^{11}	4×10^{11}	1.1×10^{11}
249.62	140–150	8.94–8.28	4×10^{12}	6×10^{12}	2.3×10^{12}
	150–168	8.28–7.40	1×10^{13}	1.8×10^{13}	4×10^{12}

rapidly with wavelength in these regions, a particular gas mix will only give enhanced conversion efficiency over a very narrow range of wavelengths, generally much less than one nanometer [5].

To measure the effectiveness of gas mixing near xenon resonances a series of experiments were done in which the VUV was set to a fixed wavelength and gas mixtures with fixed partial pressures of xenon and argon were slowly leaked into the four wave mixing cell. Typically the maximum VUV output for a given wavelength occurred at a total gas pressure more than twice the optimal pressure seen for pure xenon gas. In Fig. 4 the compositions of the gas mixtures giving optimal VUV output are shown. Four wave mixing efficiencies were enhanced over pure xenon by up to a factor of three.

In addition to the xenon resonances, the tuning range of the VUV source includes a resonance in krypton gas at 123.58 nm. By taking advantage of the anomalous dispersion of krypton gas at the high energy side of this resonance, mixtures of krypton and xenon can enhance the conversion efficiency at wavelengths shorter than 123.58 nm. The compositions of the krypton and xenon mixtures that give optimal conversion efficiencies are also shown in Fig. 4. For these mixtures gains were more modest, with VUV outputs increased by approximately 30% compared to pure xenon.

3.1.3. Spectral purity

The single MgF_2 lens used to disperse the VUV, UV, and visible or IR wavelengths involved in the four wave mixing process gives good separation of the VUV and pump beams with a minimum of optical elements. This allows the UV and visible or IR light to be blocked by a ceramic beam dump while the VUV light passes through a pinhole and is directed into the mass spectrometer. Fig. 5 shows calculated edge to edge separations between the UV and VUV beams, based on the 2σ beam waist of the input UV laser beam (calculations done with OSLO 6.4.4, Lambda Research Corp). Separation is always larger than the blocker pinhole radius (1.5 mm), ensuring proper discrimination at all wavelengths. Also shown in Fig. 5 is a digital photograph of the ceramic blocker fully inserted into the path of the three laser beams (visible, UV, and VUV). By using the two-photon xenon resonance at 249.62 nm and 355 nm light for the mixing, VUV light at 193 nm was generated. Light at 193 nm not only gives decent fluorescence intensity on the blocker, but also represents the lower limit of achievable separation.

Although the wavelength separation of the monochromator is very good, some scattered UV light does enter the ion trap. The scattered UV light can be measured directly by the same phototube that is used for the VUV (the sensitivity of the tube in the UV is in fact significantly higher than in the VUV). In Fig. 3 the UV entering the trap is shown as a grey trace. In all cases, measured UV powers were at least eight orders of magnitude lower than the input power, proving the effectiveness of the monochromator. For the UV measurements, the error from interpolation of the phototube calibration curve is negligible, so the total uncertainty of 25% for the UV values in Fig. 3 stems exclusively from uncertainty in the reflectance of the MgF_2 window.

The presence of the UV background has no discernable effect on single photon ionization. No ions are detected if the light from the OPO is blocked and only the UV background is allowed into the ion trap. This is true even for aromatic compounds which have strong REMPI cross-sections in the UV. Also, for all of the species analyzed,

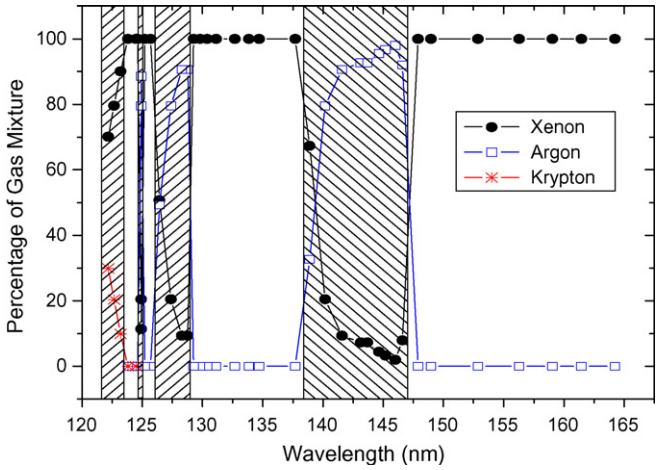

Fig. 4. Composition [in vol%] of the gas mixtures used for four wave mixing throughout the full energy range of the VUV source. On the high energy side of the xenon resonances (at 147.0, 129.6 and 125.0 nm) mixtures of xenon and argon are used. On the high energy side of the krypton resonance (at 123.6 nm) a mixture of krypton and xenon is used. Shaded regions mark areas where gas mixing can be used to enhance the VUV production.

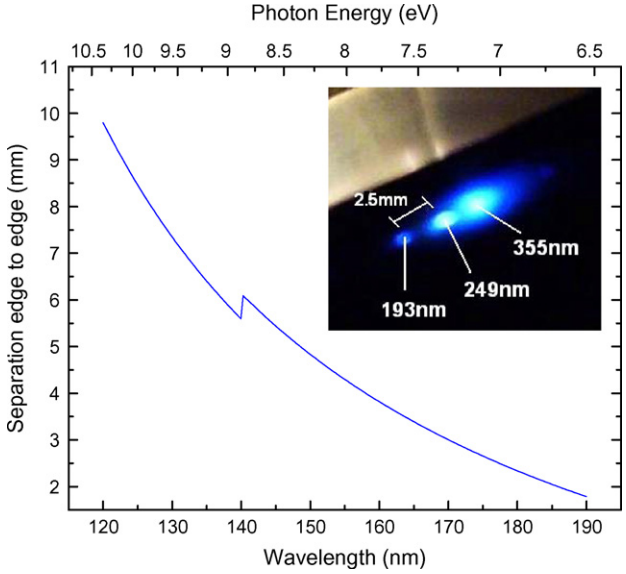

Fig. 5. Calculated monochromator performance as measured by the separation of the VUV and UV laser beam *edges* at the ceramic blocker. The photograph in the inset shows the actual fluorescence of the blocker from dispersed 355 nm, 249 nm, and 193 nm light. Even in this worst case scenario, where the dispersion from the MgF_2 lens is weakest, good separation of the beams is achieved and experiment and model agree fairly well.

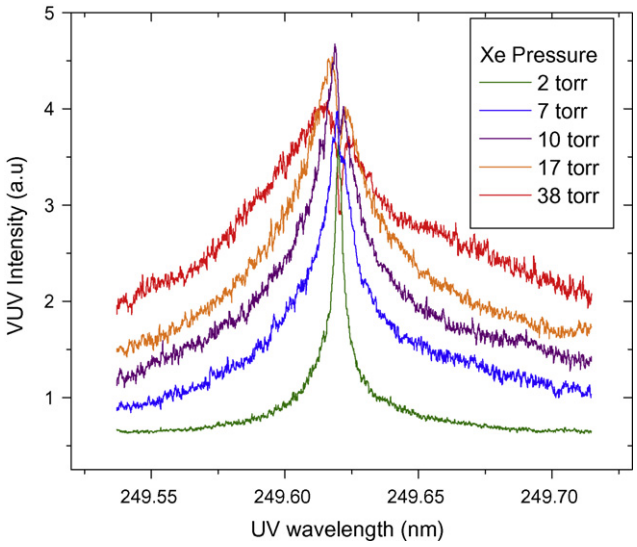

Fig. 6. Pressure broadening of the 249.62 nm two-photon resonance in xenon gas. For this experiment the tunable wavelength was set at 533 nm (giving a VUV wavelength of 163 nm). Xenon gas pressures were 2, 7, 10, 17, and 38 Torr. At higher gas pressures phase matching cannot be achieved at the center of the resonance, and considerable pressure broadening is seen.

the onset of ionization observed by scanning the VUV energy was very close to the literature value for the ionization threshold, suggesting that the ionized molecules are not absorbing UV photons in addition to VUV photons.

3.1.4. Stability

The stability of the VUV source over time is highly dependent on keeping the dye laser tuned to the exact two-photon resonance being used. Fortunately broadening of the resonance can virtually eliminate the effects of small drifts in the UV wavelength. Fig. 6 shows the effect of increasing the xenon pressure in the rare gas cell. At pressures between 7 Torr and 38 Torr the resonance becomes considerably broadened. At 17 Torr a small dip appears at the peak of the profile. This occurs because phase matching can no longer be maintained at the center of the resonance [63]. At pressures greater than 50 Torr VUV conversion efficiency begins to decline. However, moderate gas pressures do not reduce the amount of VUV produced, and the broadening of the resonance at these pressures helps to increase the stability of the system over time. As a result of this broadening the grating in the dye laser can be left for days before it needs to be re-optimized.

In addition to pressure broadening, the high intensity of the UV pulses gives rise to power broadening of the two-photon resonance, which also helps to stabilize the system.

In theory the VUV intensity should also be quite sensitive to small drifts in the power of the UV and visible/IR pulses. However, it was observed that increasing the output of either the dye laser or the OPO beyond a certain point had a negligible effect on the VUV production. Although this effectively limits the amount of VUV that can be generated by the system, it does help to give relatively constant VUV intensities over the entire wavelength range since small changes in the intensity of the OPO output as it is scanned do not have an overwhelming impact on the VUV intensity. This also helps explain why the shot-to-shot variability of the VUV power (~10%) is considerably less than the sum of the power variations of the input lasers (~8% per laser).

3.2. Ionization of gas phase organics

Seven different organic species were analyzed in the gas phase in order to test the effectiveness of the VUV system as a soft ionization source for mass spectrometry. The linearity of the technique was assessed, and both photoionization efficiency curves and SPI mass spectra were collected for all seven organics (Table 3).

Shot-to-shot variability in the ion signal was approximately 66%, arising mainly from fluctuations in the ion trapping efficiency. It is likely that these fluctuations arose from the fact that no effort was made to optimize the phase angle of the RF potential for efficient trapping at the time that the ions were generated. It has been shown that the phase angle of the RF potential to which injected ions are first exposed can have a large impact on the efficiency with which they are trapped [64,65]. Since the phase angle of the RF potential was essentially random with respect to the firing of the lasers, some shots would have generated ions at more opportune phase angles than others, leading to large variations in the trapping efficiency. In future experiments an attempt will be made to synchronize the phase angle of the RF potential with the VUV pulses. However, not all of the variability in the ion signal was due to fluctuations in the trapping efficiency. Variability in the VUV intensity (approximately 10% shot-to-shot) and small fluctuations in the response of the ion detector also contributed.

The linearity of the instrument's response was tested with respect to both the VUV intensity and the amount of analyte present. A linear response to changing VUV intensity makes it possible to normalize the ion signal to the VUV photon flux. A linear response to the amount of analyte present means that quantitative studies may be possible. To test the VUV intensity dependence, tripropyl amine was ionized at 8.17 eV (152 nm). At 8.17 eV the photon flux of the VUV source is high, giving a good dynamic range over which to test the response of the system. To test the linearity of the system with respect to the amount of analyte present, benzene gas was ionized at 10.02 eV (124 nm). In both cases a linear response was seen (Fig. 7). The larger errors for the benzene number density in Fig. 7(b) reflect the uncertainty in the reproducibility of the cold cathode gauge (5% is reported by the manufacturer) and the uncertainty in its calibration. The plot of ion signal versus benzene number density can be used to calculate a gas phase detection limit for benzene ionized at 10.02 eV. If a detection limit of three times the standard deviation of the noise is used, the sin-

Table 3
Neutral molecule masses, literature IE values, and experimental IE values for the seven gas phase organic molecules studied. Also included are the photon energies at which the mass spectra in Fig. 9 were collected.

Molecule	Molecular mass (Da)	Literature IE (eV)	Experimental IE determined by linear extrapolation of the threshold region of the PIE curve (eV)	Photon energy to obtain the mass spectrum in Fig. 9 (eV)
Benzene	78.11	9.24378 ± 0.00007 [50]	9.22 ± 0.05	10.12
Toluene	92.14	8.828 ± 0.001 [50]	8.80 ± 0.02	8.84
Chlorobenzene	112.56	9.07 ± 0.02 [50]	9.04 ± 0.02	9.18
Ethylbenzene	106.17	8.77 ± 0.01 [50]	8.74 ± 0.02	8.82
Benzaldehyde	106.12	9.50 ± 0.08 [50]	9.50 ± 0.02	9.54
α-Pinene	136.23	8.07 [81]	8.13 ± 0.10	8.18
Tripropyl amine	143.27	7.23 [83]	7.44 ± 0.10	7.5

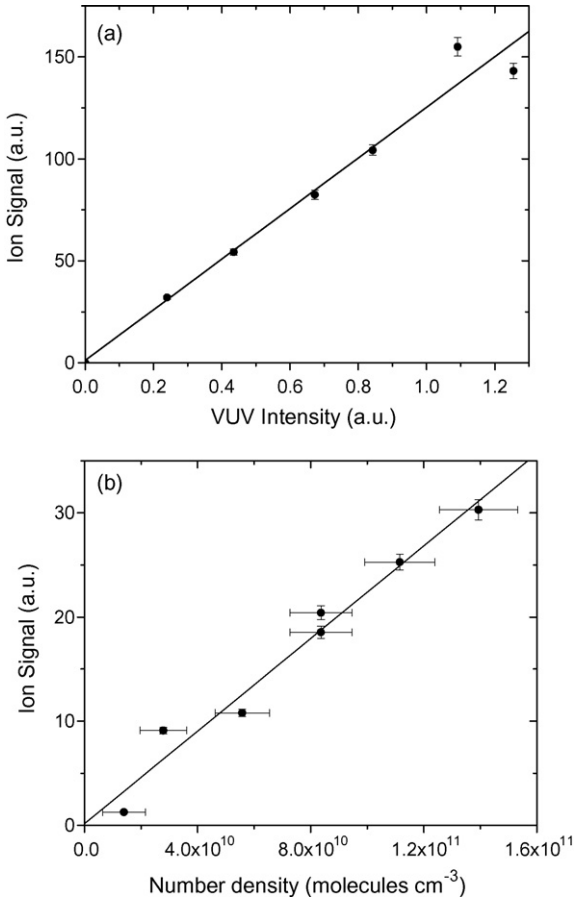

Fig. 7. Total ion signal with respect to (a) VUV intensity and (b) analyte pressure. VUV intensity dependence was measured using tripropyl amine and a photon energy of 8.17 eV (152 nm). Analyte pressure dependence was measured using benzene and a photon energy of 10.02 eV (124 nm).

gle shot gas detection limit for benzene at this photon energy is $4.2 \times 10^9 \pm 3 \times 10^9$ molecules cm^{-3}.

The ability to obtain photoionization efficiency curves and to observe the appearance energy of ions is a distinct advantage of a tunable VUV system. This information can facilitate the identification of unknown species and can provide a useful tool for determining the composition of a mixture. A group working at the Advanced Light Source at Berkeley National Labs has used PIE curves obtained with the tunable VUV light from a synchrotron source to identify components of atmospheric aerosols [42] and to determine their ionization energies [42,43]. Another group working at the same facility has done considerable work using tunable VUV to study combustion chemistry. They have been able to measure photoionization cross-sections, determine ionization energies, and, by comparison of observed ionization energies with calculated values, identify many of the species involved in combustion chemistry [66–74].

In this study photoionization efficiency curves were obtained for seven gas phase organic molecules with ionization energies spanning the full range of the VUV source (Fig. 8). To obtain the PIE curves, the VUV wavelength was scanned at a constant speed while the amount of analyte in the ion trap was held steady. A full mass spectrum was obtained for every laser shot, and the scan speed was set so that a mass spectrum was recorded every 0.001–0.002 nm. Literature values for the ionization thresholds of the seven analyzed compounds are listed in Table 3 along with the observed ionization thresholds obtained by extrapolating the linear portion of the threshold region of the PIE curves to the baseline. Despite this rather basic approach for determining the ionization threshold from the PIE curves, in almost all cases the observed onset of ionization is within 60 meV of the reported literature value. However, in most cases there is also a low energy tail that does not fall into the linear portion of the threshold, but indicates an onset of ionization at energies below the literature value for the IE. The low energy tails in Fig. 8 have a width on the order of $2kT$ (52 meV) at room temperature, and may be attributed to excitation of soft vibrational modes into the ionization continuum or to autoionizing states just below the ionization threshold. These PIE curves provide a useful test of the VUV source, and the observed onsets of ionization are close enough to the literature values that the appearance of ions at a particular energy can be used to help identify the parent molecule.

Fig. 9 shows the mass spectra obtained by setting the photon energy close to the ionization threshold of each of the seven molecules studied (photon energies used to obtain these spectra are listed in Table 3). As expected, most of the mass spectra show a parent and small isotope peak, as is the case for benzene in panel (a). Chlorobenzene in panel (c) shows two sets of peaks in the expected ratio for a compound containing both ^{35}Cl and ^{37}Cl. Toluene, however (panel (b)), shows a small peak one mass unit below the parent ion mass. Since the photon energy used for toluene ionization was well below the appearance energy of either tropylium or benzylium ions [75], it seems unlikely that direct photodissociation would be causing the $[M-H]^+$ ion to appear. Instead, we believe that collisional processes in the ion trap are responsible. This theory was tested by increasing the RF storage voltage, thereby increasing the kinetic energy of the stored ions during the cooling phase which in turn increases the collisional energy and hence the likelihood of fragmentation. For toluene, this increase in the storage voltage led to a factor of four increase in the ratio of the $[M-H]^+$ ion to the parent ion. The same effect can be observed for benzaldehyde (panel (e)) and tripropylamine (panel (g)). These cases show that collisional process in the ion trap can at times offset some of the benefits gained by near threshold ionization.

A tunable VUV source has a significant advantage over single photon ionization sources operated at a fixed energy, typically 10.5 eV, since the ability to tune the ionization energy can minimize and, in some cases, completely eliminate fragmentation of the parent ion [39]. In these experiments tripropyl amine showed no fragmentation near the ionization threshold, but began to show a significant amount of fragmentation when the photon energy was increased by as little as 0.5 eV. By the time it was raised by 1.5 eV to reach an energy of 10 eV, the parent ion made up less than 35% of the total ion signal. This is shown in panels (g) and (g′) of Fig. 9.

The ability to obtain fragment free, or nearly fragment free, mass spectra has several advantages. For mixtures of compounds it leads to much simpler spectra than those obtained with conventional ionization techniques such as electron impact. In addition, compounds that have very similar fragmentation patterns might be more readily distinguished if only the parent peak is present. On the other hand, electron impact has an advantage in that often the fragmentation pattern gives additional chemical information that is not available from a mass spectrum containing only the parent peak. However, by using a soft ionization source coupled to an ion trap mass spectrometer it is possible to selectively trap a parent ion of interest and perform MS/MS, thereby regaining the chemical information sacrificed by soft ionization.

3.3. Single particle measurements

As a first test of the applicability of the VUV source to organic aerosol mass spectrometry, experiments with caffeine particles were undertaken. Fig. 10 shows a series of mass spectra from

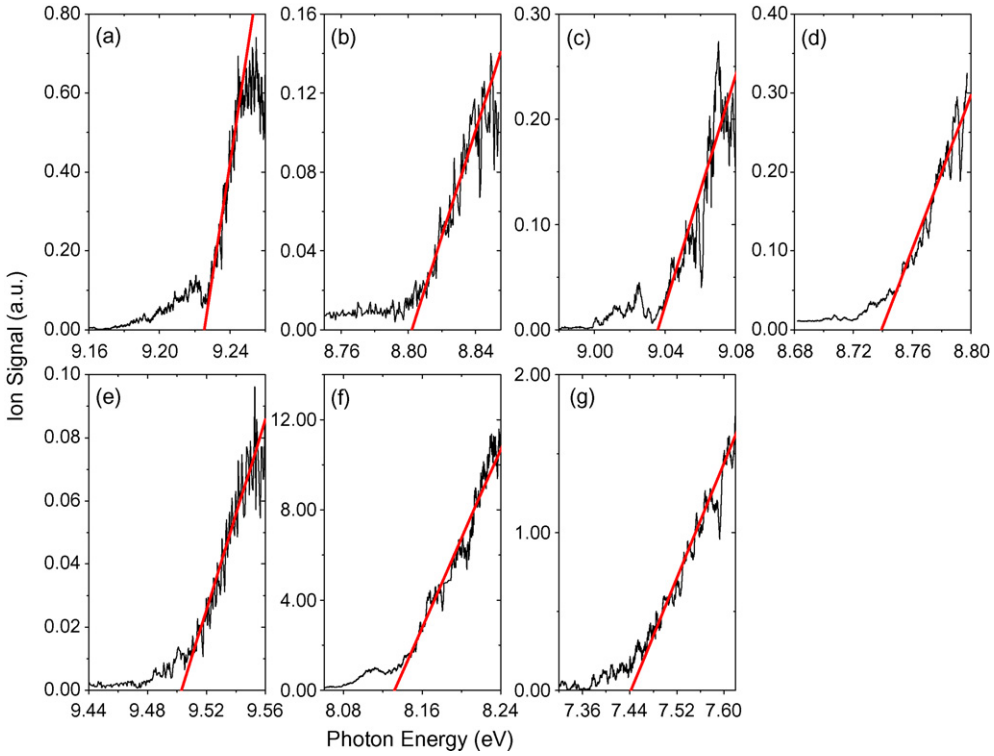

Fig. 8. Photoionization efficiency curves showing the onset of ionization for (a) benzene, (b) toluene, (c) chlorobenzene, (d) ethylbenzene, (e) benzaldehyde, (f) α-pinene, and (g) tripropyl amine. Linear fits were used to extrapolate the experimental onset of ionization from the linear portion of the curve. Onsets of ionization are listed in Table 3.

650 nm particles vaporized at CO_2 laser energies of 5, 10, 15, and 20 mJ and ionized 3 μs later by 142 nm (8.75 eV) VUV radiation. The CO_2 laser is tunable across 60 rotational lines between 923 cm^{-1} and 1087 cm^{-1} (10.8–9.2 μm) and for these experiments it was tuned to 978 cm^{-1} (10.22 μm), which corresponds to a small IR absorption band in caffeine [76]. The mass spectra show that the parent ion remains dominant over the full extent of our CO_2 energy range; however, fragments begin to appear at energies above 10 mJ/pulse. The main fragment is at m/z 109 with lower abundance fragments at m/z 193, 165, 137, 82, and a very small peak at m/z 94. These peaks are well known from literature caffeine mass spectra obtained using 70 eV electron impact [77]. The appearance of fragments with increased heating of the aerosol during vaporization is not surprising and is in agreement with results reported for the vaporization of particles using both pulsed IR lasers and impaction on a heated probe [39,40,78,79]. The dynamics of aerosol heating by the CO_2 laser pulse will be the focus of a future publication. However, Fig. 10 does shows that high quality aerosol mass spectra can be obtained with our new VUV system. In addition, if the vaporization laser energy is kept reasonably low, fragment

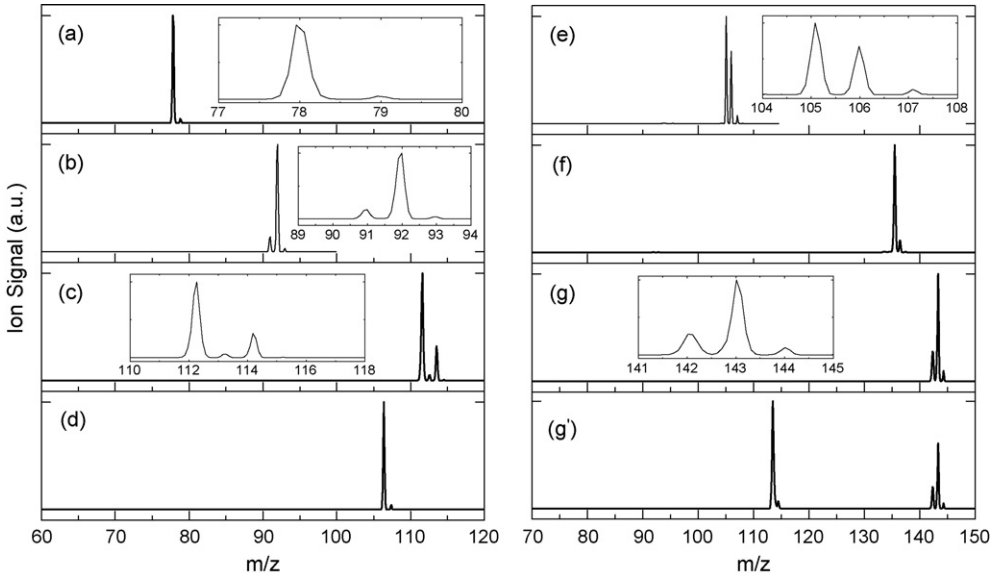

Fig. 9. Single photon ionization mass spectra of (a) benzene, (b) toluene, (c) chlorobenzene, (d) ethylbenzene, (e) benzaldehyde, (f) α-pinene, (g) tripropyl amine ionized with with 7.5 eV, and (g′) tripropyl amine ionized with 10 eV. The photon energies at which spectra (a) through (g) were collected are listed in Table 3.

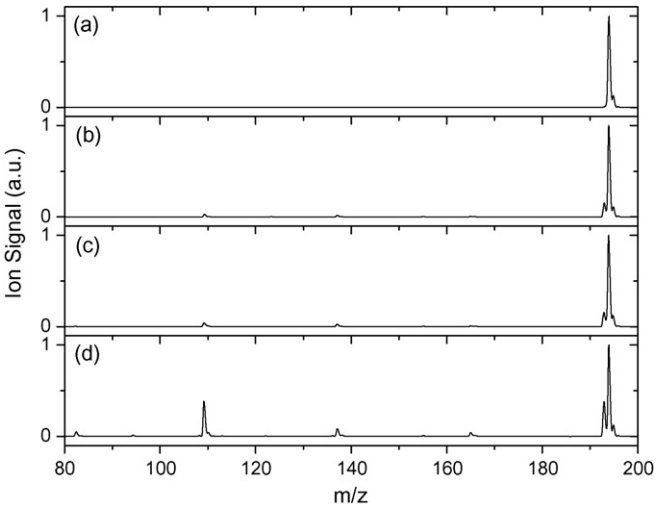

Fig. 10. Caffeine aerosol mass spectra as a function of the CO_2 laser energy used to vaporize the particles. The particles used for these experiments were 650 nm in diameter and the vaporization energies were (a) 5 mJ/p, (b) 10 mJ/p, (c) 15 mJ/p, and (d) 20 mJ/p.

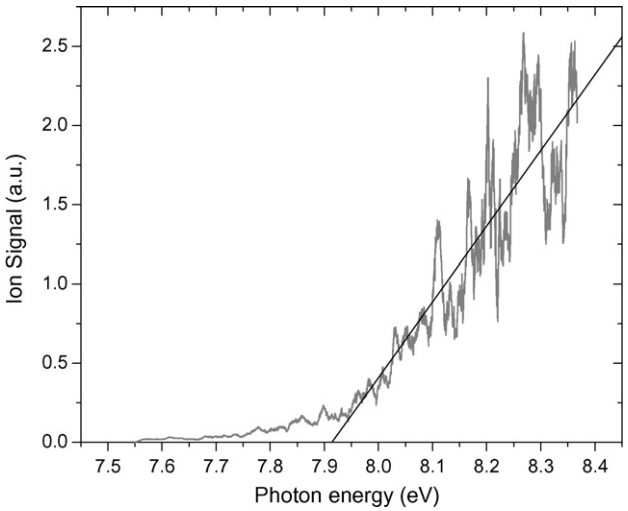

Fig. 12. Photoionization efficiency curve for caffeine. The extrapolated appearance energy for caffeine is 7.91 ± 0.05 eV.

free mass spectra can be obtained. Fig. 11 shows mass spectra from 300 nm caffeine particles which were vaporized with 15 mJ of 978 cm^{-1} infrared light and ionized by 142 nm (8.75 eV) VUV light after a delay of 3 μs. The top frame is an average of 200 laser shots and the bottom frame is a single particle. Both the averaged and single particle spectra have very good signal to noise ratios. If a detection limit of three times the standard deviation of the noise is used, we can calculate a minimum detectable particle diameter of 75 nm for caffeine from the averaged spectrum. Analyzing particles this small is not possible at present since we cannot detect scattered light from caffeine particles below ~225 nm in the aerosol timing and sizing region, however this detection limit should allow for detection of low concentration components in larger aerosol particles. With caffeine, for example, we should be able to detect down to 8×10^5 molecules which is approximately 1.5% of a 300 nm particle.

Fig. 12 is a photoionization efficiency curve for pure caffeine aerosols 550 nm in diameter. The solid line was obtained by continuously scanning the VUV wavelength and recording both the ion signal and the VUV power for each laser shot. Scan speeds were on the order of 0.005 nm/s (0.0003 eV/s at 140 nm) and spectra were recorded 3–4 times per second to give a resolution of ~0.002 nm (0.0001 eV). Fluctuations in the VUV intensity were compensated for by normalizing the ion signal to the recorded VUV intensity for each laser shot. An extrapolation of the linear portion of the PIE curve gives an appearance energy for caffeine of 7.91 ± 0.05 eV. The IE of caffeine has been reported as both 7.95 eV [80] and 8.50 eV [81]. This is the first measurement of ionization energies of aerosol constituents using a laser based VUV source.

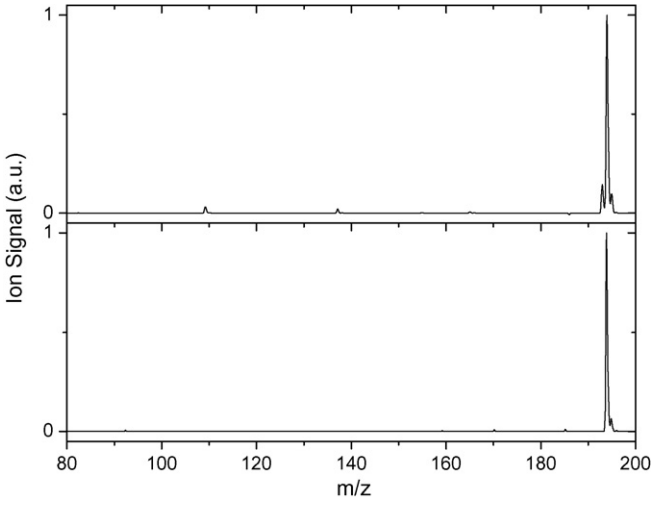

Fig. 11. Mass spectra from 300 nm caffeine particles vaporized by 15 mJ of CO_2 laser energy (978 cm^{-1}) and ionized with 142 nm VUV after 3 μs. The top panel is an average of 200 shots while the bottom is a single particle.

3.4. Sensitivity to other aerosol types

Our ability to detect various other organic aerosol constituents will be a function of several factors. The degree of vaporization from the CO_2 laser will affect the number of molecules that are available in the gas phase for ionization. This has not been explored in this work, but the effects of varying the vaporization parameters will be discussed in future publications. There are also several factors which will affect the ionization efficiency of the molecules once they are in the gas phase. Obviously the ionization energy must be in the range that is accessible with our VUV source (7.4–10.2 eV). For aerosol particles, which are generally composed of larger non-volatile or semi-volatile molecules, most relevant organics with be accessible. Adam et al. have plotted homologue series of several organic compound classes as a function of ionization energy [82]. In general, the ionization energy decreases as the molecular mass increases. Alkanes with greater than five carbons have ionization energies below 10.2 eV, aldehydes with greater than three carbons have IEs below 10 eV, and alkenes with greater than two carbons have IEs below 9.8 eV [82], all of which are within the accessible range of our VUV source. Alkynes and alcohols with greater than four carbons tend to have ionization energies below 10.2 eV [82], but the trend toward lower IEs at higher masses is much weaker for these molecules, which means that shorter VUV wavelengths, where our photon flux is weaker, must be used even for larger molecules. Several larger carboxylic acids, such as oleic, linolenic, and linoleic acid, have IEs in the accessible range (8.52–8.69 eV) [43]. Hexanoic (≤10.12 eV) and butanoic acid (10.17 eV) are within reach [50], but small acids such as acetic acid (10.65 eV) and formic acid (11.33 eV) are not accessible. Ketones

and aromats of most sizes should be accessible (IE's below 10 eV) [82].

Another factor which will affect the ionization efficiency of the gas phase aerosol constituents is the photoionization cross-section. Although SPI is an almost universal ionization method, the photoionization cross-sections for different molecule classes can differ by close to a factor of ten at a given wavelength [82]. For example, the photoionization cross-section of benzene at 118 nm (10.49 eV) is measured as 22 Mb while the cross-section of decane is 3.7 Mb [82]. In addition, the photoionization cross-section increases as the ionizing energy is increased for the first few electron volts beyond the ionization threshold. As a result, a lower detection limit for a particular molecule is possible if a photon energy well above its IE is used for ionization, but this may come at the expense of increased fragmentation.

Arguably the most important factor in determining our detection limit for a particular molecule is the photon flux available at the energy to be used for ionization. For our source, a change in the photon flux of over three orders of magnitude between 122 nm and 168 nm will have a significant impact on the detection limit for molecules with high IEs.

As a worst case scenario, we can consider a hypothetical molecule which we would ionize at 123 nm (10.10 eV) where the photon flux is $\sim 8 \times 10^9$ photons/pulse, roughly 300 times less than for our caffeine measurements at 142 nm. We will assume that the molecular mass and density are similar to caffeine, so that a similar number of molecules make up an aerosol particle of any given size. If the photoionization cross-section is the same as that of caffeine, our detection limit would be a pure 500 nm particle, or a 10% component of a 1 μm particle. Our instrument has been initially developed for laboratory studies of heterogeneous chemistry, and a detection limit of 10% of a 1 μm particle is still adequate for many experiments. If we assume a worst case scenario where the photoionization cross-section is an order of magnitude lower, we would have a detection limit of a pure 1 μm particle. In this case we would be limited to a VUV wavelength of 130 nm to 168 nm (9.56–7.40 eV) where our photon flux is higher. Future experiments will explore the applicability of the VUV source to a variety of compound classes.

4. Conclusions

A continuously tunable VUV source based on resonance enhanced four wave difference mixing in xenon gas has been constructed and characterized. The source produces narrow bandwidth, high intensity pulses of light between 122 nm (10.2 eV) and 168 nm (7.4 eV), and could readily be applied to a wide variety of mass spectrometry based experiments. Very high spectral purity is achieved with a custom monochromator based around a single MgF_2 lens. Currently, the VUV source is coupled to an ion trap mass spectrometer which has also been fitted with an aerosol interface to conduct single particle mass spectrometry experiments. Aerosol experiments were carried out using caffeine particles. Under appropriate vaporization conditions fragment free mass spectra were collected for single aerosol particles as small as 300 nm in diameter. Excellent signal to noise characteristics for these small particles give a caffeine detection limit of 8×10^5 molecules which is equivalent to a single 75 nm aerosol, or approximately 1.5% of a 300 nm particle. A good photon flux across the full wavelength range of the VUV source should allow the instrument to be used to study the heterogeneous chemistry of many types of organic aerosols of atmospheric relevance. The continuous tunability of the VUV source also allows the components of aerosol particles to be identified by the appearance energies of their ions.

Acknowledgements

We would like to thank Dr. Saeid Kamal for providing his technical expertise in the lab, and Dr. Valery Milner for his very helpful discussions during the design and construction of the VUV monochromator. Many thanks also to the personnel of the mechanical and electrical shops in the UBC chemistry department, whose expertise was invaluable.

This work was carried out in the UBC Laboratory for Advanced Spectroscopy and Imaging Research (LASIR). Funding for this project was provided by the National Sciences and Engineering Council of Canada (NSERC), the Canadian Foundation for Climate and Atmospheric Sciences (CFCAS), the Canadian Foundation for Innovation (CFI), the British Columbia Knowledge Development Fund (BCKDF), and the NRC-NSERC-BDC Nanotechnology Initiative.

References

[1] D.J. Butcher, D.E. Goeringer, G.B. Hurst, Anal. Chem. 71 (1999) 489.
[2] F. Mühlberger, J. Wieser, A. Morozov, A. Ulrich, R. Zimmermann, Anal. Chem. 77 (2005) 2218.
[3] K.R. Wilson, L. Belau, C. Nicolas, M. Jimenez-Cruz, S.R. Leone, M. Ahmed, Int. J. Mass Spectrom. 249 (2006) 155.
[4] S. Kuribayashi, H. Yamakoshi, M. Danno, S. Sakai, S. Tsuruga, H. Futami, S. Morii, Anal. Chem. 77 (2005) 1007.
[5] S.E. Vanbramer, M.V. Johnston, Appl. Spectrosc. 46 (1992) 255.
[6] J.W. Hepburn, in: A.B. Myers, T.R. Rizzo (Eds.), Generation of Coherent Vacuum Ultraviolet Radiation: Applications to High-Resolution Photoioniztion and Photoelectron Spectroscopy, John Wiley and Sons Inc., New York, 1995, p. 149.
[7] C.R. Vidal, in: L.F. Mollenauer, J.C. White (Eds.), Four-Wave Frequency Mixing in Gases, Springer-Verlag, Berlin, 1979.
[8] R.H. Lipson, in: D.L. Andrews, A.A. Demidov (Eds.), Tunable Short Wavelength Generation and Applications, Kluwer Academic, New York, 2002, p. 257.
[9] R.H. Lipson, S.S. Dimov, P. Wang, Y.J. Shi, D.M. Mao, X.K. Hu, J. Vanstone, Instrum. Sci. Technol. 28 (2000) 85.
[10] G. Hilber, A. Lago, R. Wallenstein, J. Opt. Soc. Am. B-Opt. Phys. 4 (1987) 1753.
[11] G.W. Faris, S.A. Meyer, M.J. Dyer, M.J. Banks, J. Opt. Soc. Am. B-Opt. Phys. 17 (2000) 1856.
[12] F. Qi, A. McIlroy, Combust. Sci. Technol. 177 (2005) 2021.
[13] J.B. Pallix, U. Schuhle, C.H. Becker, D.L. Huestis, Anal. Chem. 61 (1989) 805.
[14] O. Kornienko, E.T. Ada, J. Tinka, M.B.J. Wijesundara, L. Hanley, Anal. Chem. 70 (1998) 1208.
[15] E. Nir, H.E. Hunziker, M.S. de Vries, Anal. Chem. 71 (1999) 1674.
[16] F. Mühlberger, R. Zimmermann, A. Kettrup, Anal. Chem. 73 (2001) 3590.
[17] W.A. Vondrasek, S. Okajima, J.P. Hessler, Appl. Optics 27 (1988) 4057.
[18] B.J. Finlayson-Pitts, J.N. Pitts Jr., Chemistry of the Upper and Lower Atmosphere: Theory, Experiments, and Applications, Academic Press, New York, 2000.
[19] M. Kanakidou, J.H. Seinfeld, S.N. Pandis, I. Barnes, F.J. Dentener, M.C. Facchini, R. Van Dingenen, B. Ervens, A. Nenes, C.J. Nielsen, E. Swietlicki, J.P. Putaud, Y. Balkanski, S. Fuzzi, J. Horth, G.K. Moortgat, R. Winterhalter, C.E.L. Myhre, K. Tsigaridis, E. Vignati, E.G. Stephanou, J. Wilson, Atmosph. Chem. Phys. 5 (2005) 1053.
[20] J.J. Schauer, W.F. Rogge, L.M. Hildemann, M.A. Mazurek, G.R. Cass, Atmos. Environ. 30 (1996) 3837.
[21] J.J. Schauer, G.R. Cass, Environ. Sci. Technol. 34 (2000) 1821.
[22] K.P. Hinz, B. Spengler, J. Mass Spectrom. 42 (2007) 843.
[23] M.C. Jacobson, H.C. Hansson, K.J. Noone, R.J. Charlson, Rev. Geophys. 38 (2000) 267.
[24] D.M. Murphy, Mass Spectrom. Rev. 26 (2007) 150.
[25] D.G. Nash, T. Baer, M.V. Johnston, Int. J. Mass Spectrom. 258 (2006) 2.
[26] R.C. Sullivan, K.A. Prather, Anal. Chem. 77 (2005) 3861.
[27] M.R. Canagaratna, J.T. Jayne, J.L. Jimenez, J.D. Allan, M.R. Alfarra, Q. Zhang, T.B. Onasch, F. Drewnick, H. Coe, A. Middlebrook, A. Delia, L.R. Williams, A.M. Trimborn, M.J. Northway, P.F. DeCarlo, C.E. Kolb, P. Davidovits, D.R. Worsnop, Mass Spectrom. Rev. 26 (2007) 185.
[28] B.W. LaFranchi, G.A. Petrucci, Int. J. Mass Spectrom. 258 (2006) 120.
[29] J.D. Hearn, G.D. Smith, Anal. Chem. 76 (2004) 2820.
[30] W.A. Harris, P.T.A. Reilly, W.B. Whitten, Anal. Chem. 79 (2007) 2354.
[31] B.D. Morrical, D.P. Fergenson, K.A. Prather, J. Am. Soc. Mass Spectr. 9 (1998) 1068.
[32] A. Zelenyuk, J. Cabalo, T. Baer, R.E. Miller, Anal. Chem. 71 (1999) 1802.
[33] A. Zelenyuk, D. Imre, Aerosol Sci. Technol. 39 (2005) 554.
[34] A. Lazar, P.T.A. Reilly, W.B. Whitten, J.M. Ramsey, Environ. Sci. Technol. 33 (1999) 3993.
[35] M. Bente, T. Adam, T. Ferge, S. Gallavardin, M. Sklorz, T. Streibel, R. Zimmermann, Int. J. Mass Spectrom. 258 (2006) 86.
[36] E. Woods, G.D. Smith, Y. Dessiaterik, T. Baer, R.E. Miller, Anal. Chem. 73 (2001) 2317.
[37] B. Oktem, M.P. Tolocka, M.V. Johnston, Anal. Chem. 76 (2004) 253.

[38] T. Ferge, F. Mühlberger, R. Zimmermann, Anal. Chem. 77 (2005) 4528.
[39] D.G. Nash, X.F. Liu, E.R. Mysak, T. Baer, Int. J. Mass Spectrom. 241 (2005) 89.
[40] M.J. Northway, J.T. Jayne, D.W. Toohey, M.R. Canagaratna, A. Trimborn, K.I. Akiyama, A. Shimono, J.L. Jimenez, P.F. DeCarlo, K.R. Wilson, D.R. Worsnop, Aerosol Sci. Technol. 41 (2007) 828.
[41] J.N. Shu, S.K. Gao, Y. Li, Aerosol Sci. Technol. 42 (2008) 110.
[42] E. Gloaguen, E.R. Mysak, S.R. Leone, M. Ahmed, K.R. Wilson, Int. J. Mass Spectrom. 258 (2006) 74.
[43] E.R. Mysak, K.R. Wilson, M. Jimenez-Cruz, M. Ahmed, T. Baer, Anal. Chem. 77 (2005) 5953.
[44] J.N. Shu, K.R. Wilson, M. Ahmed, S.R. Leone, Rev. Scientific Instrum. 77 (2006).
[45] K.R. Wilson, M. Jimenez-Cruz, C. Nicolas, L. Belau, S.R. Leonet, M. Ahmed, J. Phys. Chem. A 110 (2006) 2106.
[46] J. Wieser, D.E. Murnick, A. Ulrich, H.A. Huggins, A. Liddle, W.L. Brown, Rev. Scientific Instrum. 68 (1997) 1360.
[47] F. Mühlberger, J. Wieser, A. Ulrich, R. Zimmermann, Anal. Chem. 74 (2002) 3790.
[48] S.E. Vanbramer, M.V. Johnston, J. Am. Soc. Mass Spectr. 1 (1990) 419.
[49] Y.J. Shi, R.H. Lipson, Can. J. Chem. 83 (2005) 1891.
[50] S.G. Lias, in: P.J. Linstrom, W.G. Mallard (Eds.), Ionization Energy Evaluation, National Institute of Standards and Technology, Gaithersburg, MD, 2005.
[51] T. Kobayashi, K. Yokota, S. Nagakura, Bull. Chem. Soc. Japan 48 (1975) 412.
[52] Y.M. Li, H.Y. Li, Q. Sun, D.X. Wang, Acta Chim. Sinica 61 (2003) 1492.
[53] P. Rupper, F. Merkt, Rev. Scientific Instrum. 75 (2004) 613.
[54] J.W. Hepburn, in: C.Y. Ng (Ed.), Applications of Coherent Vacuum Ultraviolet to Photofragment and Photoionization Spectroscopy, World Scientific Publishing Co. Pte. Ltd, Singapore, 1991.
[55] A.A. Specht, M.W. Blades, J. Am. Soc. Mass Spectr. 14 (2003) 562.
[56] D. Robb, M.W. Blades, J. Am. Soc. Mass Spectr. 8 (1997) 1203.
[57] E.A. Simpson, P. Campuzano-Jost, S.J. Hanna, D.B. Robb, J.H. Hepburn, M.W. Blades, A.K. Bertram, Int. J. Mass Spectrom., submitted.
[58] P. Liu, P.J. Ziemann, D.B. Kittelson, P.H. McMurry, Aerosol Sci. Technol. 22 (1995) 314.
[59] P. Liu, P.J. Ziemann, D.B. Kittelson, P.H. McMurry, Aerosol Sci. Technol. 22 (1995) 293.
[60] M.W. Williams, R.A. Macrae, E.T. Arakawa, J. Appl. Phys. 38 (1967) 1701.
[61] R. Mahon, T.J. Mcilrath, V.P. Myerscough, D.W. Koopman, IEEE J. Quantum Electron. 15 (1979) 444.
[62] R. Hilbig, R. Wallenstein, IEEE J. Quantum Electron. 17 (1981) 1566.
[63] R. Hilbig, R. Wallenstein, IEEE J. Quantum Electron. 19 (1983) 194.
[64] L. He, D.M. Lubman, Rapid Commun. Mass Spectrom. 11 (1997) 1467.
[65] C. Weil, M. Nappi, C.D. Cleven, H. Wollnik, R.G. Cooks, Rapid Commun. Mass Spectrom. 10 (1996) 742.
[66] T.A. Cool, A. McIlroy, F. Qi, P.R. Westmoreland, L. Poisson, D.S. Peterka, M. Ahmed, Rev. Scientific Instrum. 76 (2005).
[67] T.A. Cool, K. Nakajima, T.A. Mostefaoui, F. Qi, A. McIlroy, P.R. Westmoreland, M.E. Law, L. Poisson, D.S. Peterka, M. Ahmed, J. Chem. Phys. 119 (2003) 8356.
[68] T.A. Cool, J. Wang, N. Hansen, P.R. Westmoreland, F.L. Dryer, Z. Zhao, A. Kazakov, T. Kasper, K. Kohse-Hoinghaus, Proc. Combust. Instit. 31 (2007) 285.
[69] T.A. Cool, J. Wang, K. Nakajima, C.A. Taatjes, A. McIlroy, Int. J. Mass Spectrom. 247 (2005) 18.
[70] N. Hansen, S.J. Klippenstein, J.A. Miller, J. Wang, T.A. Cool, M.E. Law, P.R. Westmoreland, T. Kasper, K. Kohse-Hoinghaus, J. Phys. Chem. A 110 (2006) 4376.
[71] N. Hansen, S.J. Klippenstein, P.R. Westmoreland, T. Kasper, K. Kohse-Hoinghaus, J. Wang, T.A. Cool, Phys. Chem. Chem. Phys. 10 (2008) 366.
[72] N. Hansen, J.A. Miller, C.A. Taatjes, J. Wang, T.A. Cool, M.E. Law, P.R. Westmoreland, Proc. Combust. Instit. 31 (2007) 1157.
[73] C.A. Taatjes, S.J. Klippenstein, N. Hansen, J.A. Miller, T.A. Cool, J. Wang, M.E. Law, P.R. Westmoreland, Phys. Chem. Chem. Phys. 7 (2005) 806.
[74] J. Wang, B. Yang, T.A. Cool, N. Hansen, T. Kasper, Int. J. Mass Spectrom. 269 (2008) 210.
[75] C. Lifshitz, Y. Gotkis, A. Ioffe, J. Laskin, S. Shaik, Int. J. Mass Spectrom. 125 (1993) R7.
[76] P.J. Linstrom, W.G. Mallard (Eds.), NIST Chemistry WebBook, National Institute of Standards and Technology, Gaithersburg, MD, 2005, 20899.
[77] S.E. Stein, in: P.J. Linstrom, W.G. Mallard (Eds.), Mass Spectra, National Institute of Standards and Technology, Gaithersburg MD, 2005.
[78] D.C. Sykes, E. Woods, G.D. Smith, T. Baer, R.E. Miller, Anal. Chem. 74 (2002) 2048.
[79] E. Woods, R.E. Miller, T. Baer, J. Phys. Chem. A 107 (2003) 2119.
[80] S.G. Lias, R.D. Levin, S.A. Kafafi, in: P.J. Linstrom, W.G. Mallard (Eds.), Ion Energetics Data, National Institute of Standards and Technology, Gaithersburg, MD, 2005.
[81] H.M. Rosenstock, K. Draxl, B.W. Steiner, J.T. Herron, in: P.J. Linstrom, W.G. Mallard (Eds.), Ion Energetics Data, National Institute of Standards and Technology, Gaithersburg, MD, 2005.
[82] T. Adam, R. Zimmermann, Anal. Bioanal. Chem. 389 (2007) 1941.
[83] K. Watanabe, J.R. Mottl, J. Chem. Phys. 26 (1957) 1773.